Earth and Planetary Science Letters 451 (2016) 1–9

Contents lists available at ScienceDirect

Earth and Planetary Science Letters

www.elsevier.com/locate/epsl

Setting a chronology for the basal ice at Dye-3 and GRIP: Implications for the long-term stability of the Greenland Ice Sheet

Audrey M. Yau [a], Michael L. Bender [a,b,*], Thomas Blunier [c], Jean Jouzel [d]

[a] Department of Geosciences, Princeton University, Princeton, NJ, 08540, USA
[b] Institute of Oceanology, Shanghai Jiao Tong University, 800 Dongchuan Rd., Minhang, Shanghai 200240, China
[c] Centre for Ice and Climate, Niels Bohr Institute, University of Copenhagen, Juliane Maries Vej 30, DK-2100 Copenhagen, Denmark
[d] Laboratoire des Sciences du Climat et de l'Environnement, CEA-CNRS-University Versailles-Saint Quentin, CE Saclay, Orme des Merisiers, 91191 Gif-sur-Yvette, France

ARTICLE INFO

Article history:
Received 8 March 2016
Received in revised form 23 June 2016
Accepted 26 June 2016
Available online 15 July 2016
Editor: H. Stoll

Keywords:
Greenland Ice Sheet
Dye-3
GRIP
Ar-dating
$^{17}\Delta$ stratigraphy

ABSTRACT

The long-term stability of the Greenland Ice Sheet (GIS) is an important issue in our understanding of the climate system. Limited data suggest that the northern and southern sections extend well back into the Pleistocene, but most age constraints do not definitively date the ice. Here, we re-examine the GRIP and Dye-3 ice cores to provide direct ice core observations as to whether the GIS survived previous interglacials known to be warmer (~130 ka) or longer (~430 ka) than the present interglacial. We present geochemical analyses of the basal ice from Dye-3 (1991–2035 m) and GRIP (3020–3026 m) that characterize and date the ice. We analyzed the elemental and isotopic composition of O_2, N_2, and Ar, of trapped air in these two cores to assess the origin of trapped gases in silty ice. Dating of the trapped air was then achieved by measuring the paleoatmospheric $\delta^{40}Ar/^{38}Ar$ and the ^{17}O anomaly ($^{17}\Delta$) of O_2. The resulting age is a lower limit because the trapped air may be contaminated with crustal radiogenic ^{40}Ar. The oldest average age of replicates measured at various depths is 970 ± 140 ka for the GRIP ice core and 400 ka $\pm$ 170 ka for Dye-3. $^{17}\Delta$ data from Dye-3 also argue strongly that basal ice in this core predates the Eemian. This confirms that the Greenland Ice Sheet did not completely melt at Southern Greenland during the last interglacial, nor did it completely melt at Summit Greenland during the unusually long interglacial ~430 kyr before present.

1. Introduction

The Greenland Ice Sheet is the second largest reservoir of water on land, and if completely melted, would contribute roughly 7 m to global eustatic sea level (Bamber et al., 2013). As a large, climate sensitive source to sea level rise, the response of the Greenland Ice Sheet (GIS) to global warming has been an important, debated subject. Understanding the response of the GIS to past climate change events, such as previous interglacials, can provide a more accurate context for how anthropogenic global warming may impact the GIS in the future. Here, we advance the understanding of the long-term stability of the ice sheet by dating trapped air from the base of two Greenland ice cores (Fig. 1). By dating the trapped air from the deepest ice of the GRIP ice core, located at Summit Greenland, and the Dye-3 ice core, located in Southern Greenland, we determine, from direct observations, the minimum age after which an ice sheet existed at these sites. In establishing this age, we determine whether the GIS has persisted through interglacials such as the Eemian, when Arctic temperatures were 3–5 °C warmer than today and sea level was 6–9 m higher than today (Clark and Huybers, 2009; Kopp et al., 2009) or Marine Isotope Stage 11 (400–430 ka), which was much longer than the present interglacial.

Previous studies on the trapped air in ice cores have established the antiquity of an ice sheet at Summit (GRIP and GISP2) and Northern Greenland (NEEM) through at least the last interglacial (115–130 ka), and probably back to Marine Isotope Stage 7, ~235 ka (Chappellaz et al., 1997; Suwa et al., 2006; Dahl-Jensen and Community NEEM, 2013; Yau, 2014, PhD Thesis). However, an ongoing discussion persists on the minimum age of the deepest ice at Summit Greenland (GRIP) and Southern Greenland (Dye-3) because basal ice at these sites is stratigraphically disturbed (Johnsen et al., 2001; Verbeke et al., 2002; Tison et al., 1994; Bender et al., 2010). Of particular interest is the question of whether the GIS survived at these sites through Marine Isotope Stage (MIS) 11, an

* Corresponding author at: Department of Geosciences, Princeton University, Princeton, NJ, 08540, USA.
E-mail address: bender@princeton.edu (M.L. Bender).

http://dx.doi.org/10.1016/j.epsl.2016.06.053
0012-821X/

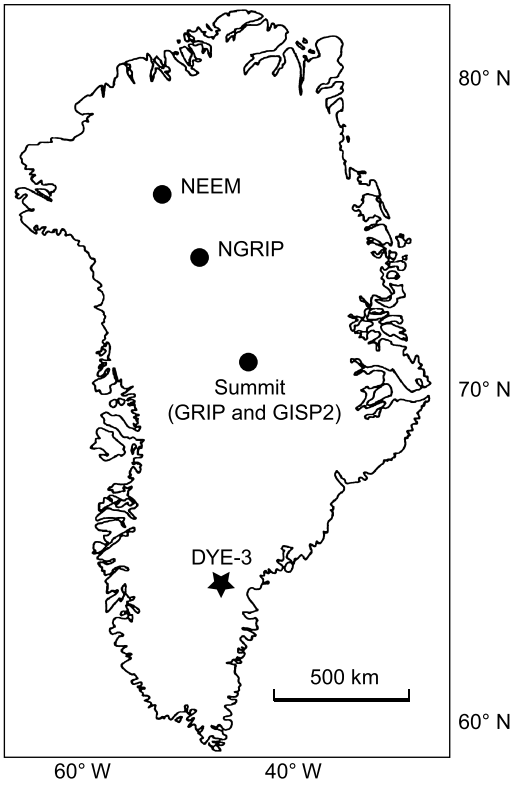

Fig. 1. Greenland ice core sites with possible Eemian-aged basal ice.

unusually long interglacial when mean global sea level may have been 6–13 m above present (Raymo and Mitrovica, 2012).

Ice at the base of the glacier has properties that originate in several different ways. "Dry densified ice" forms via the accumulation and burial of dry snow (Herron and Langway, 1980). "Wet origin ice" was partly or completely melted at some point in its history. Wet origin ice would include frozen soils, lake water, partly melted basal ice, and superimposed ice.

Dry densified ice has a total gas content of ~100 scc/kg (standard cubic centimeters of gas/kg of ice). The exact value depends on elevation (higher at low elevation), temperature (higher at colder temperatures), and summer insolation. Wet origin ice has a much lower gas content (except for metabolic CO_2 and CH_4), because the solubility of gas in water is much less than 100 scc/kg, and because gases may be exsolved upon freezing. If one mixes comparable amounts of dry densified and wet origin ice, the dry component will dominate the gas mixture. "Silty ice" sampled at the base of deep ice cores is generally dry origin ice mixed with some amount of either locally formed ice from the initial growth stages of the ice sheet (Tison et al., 1994; Souchez et al., 1994) or another basal component such as soil, permafrost, preglacial snow, lake ice, or ground ice (Bender et al., 2010). We use the term "clean ice" to describe ice free of visible silicate impurities. All clean ice samples in this paper are believed to be dry densified.

Previous studies have estimated that the silty basal ice, from 3022–3029 m depth in the GRIP ice core, could be as old as 2.4 Ma, dating to the original build-up of the GIS (Souchez et al., 1994, 2006). Souchez et al. (2006) and Tison et al. (1998) found several indications of biological activity that indicated a soil source for the silty particles found in the bottom 7 m of GRIP. These included organic matter that was present in swampy areas, drawing down the O_2 concentration to 10% of saturation, very high concentrations of methane, high concentrations of NH_4^+, and the presence of ammonium oxalate, which they attributed to the breakdown of bird droppings in local soils. They deduced that central Greenland was vegetated at the time the silty ice formed, and that traces of ancient soil were preserved in a snowdrift that was overridden by the ice sheet. $^{10}Be/^{36}Cl$ dating by Willerslev et al. (2007) gives an age of the silty basal ice of 950 ± 44 ka. The uncertainty is calculated from ^{36}Cl and ^{10}Be abundance errors only, and the authors have noted several factors that could cause the $^{36}Cl/^{10}Be$ age to be either younger or older than the true age of the ice. Here, we revisit the basal ice of the GRIP ice core to confirm the antiquity of the trapped air of this ice inferred by Souchez et al. (1994, 2006) and Willerslev et al. (2007).

Willerslev et al. (2007) also concluded that basal ice from Southern Greenland at Dye-3 is likely 450–800 ka. They presented results from a number of dating techniques (amino acid racemization, $^{10}Be/^{36}Cl$, and optical stimulated luminescence dating), each with its own set of assumptions and uncertainties, which collectively suggest that the Dye-3 silty ice dates to this age. However, the assumptions and uncertainties were large enough that Willerslev et al. (2007) were unable to conclusively rule out the possibility that the basal silty ice of Dye-3 may date only to the last interglacial (115–130 ka). Independent support for a pre-Eemian age for the southern GIS comes from sediment flux data from the southern Greenland margin (Colville et al., 2011; Reyes et al., 2014). While these studies have pointed to the antiquity and stability of the southern GIS through Arctic warm periods, earlier studies on the Dye-3 ice core inferred that the southern GIS did not persist through the Eemian. Koerner and Fisher (2002) argued that this region was ice-free during the last interglacial, as no isotopically cold ice exists below the warm basal section (Fig. 2). Other research highlights the abrupt and large increase with depth in $\delta^{18}O_{ice}$ (~8‰) over a very short interval (2012–2016 m). Koerner (1989) and Souchez et al. (1998) suggest that the silty basal ice is a completely separate unit of ice that was accreted onto the bottom of the overlying dry origin clean ice that makes up the bulk of the glacier at Dye-3 and GRIP, respectively (Fig. 2).

We analyzed samples from the clean and silty units of the Dye-3 ice core between 1991–2035 m and the GRIP ice core between 3020–3026 m. At Dye-3, $\delta^{18}O$ of the ice is nearly constant between 1990–2012 m depth at −31‰ (Holocene $\delta^{18}O = -27$‰) (Fig. 2). Silty ice first appears at ~2012 m in the Dye-3 ice core. From there to the bottom, at 2025 m depth, $\delta^{18}O$ lies in the range −24 to −26‰. At GRIP, silty ice first appears at 3022.25 m. From there to the bottom, $\delta^{18}O$ rises from about −36 to −25‰. By focusing on the trapped air in ice, we mainly characterize the dry densified ice component of the silty ice, rather than the wet origin component, which bears the silt, and has a lower total gas content (Boereboom et al., 2013). However, wet based ice, or other locally derived ice such as ice wedges, may still have substantial total gas contents (Boereboom et al., 2013). Therefore, gas ages may be aliased by wet-origin ice predating the growth of the ice sheet. Methods dating basal ice by measuring non-gas properties, such as U-series recoil dating, primarily access the wet-origin ice, and may very well give different ages.

To determine the conditions during the trapping of air, we measured the elemental and isotopic composition of O_2, N_2, and Ar. We report the composition with respect to air in the standard δ notation with units in ‰ (per mil):

$$\delta = [R/R_o - 1]$$

where δ is the fractional deviation of a gas pair ratio R from a reference (air) ratio R_o. These analyses tell us whether the trapped air has been gravitationally or thermally fractionated ($\delta^{15}N$ and $\delta^{38}Ar/^{36}Ar$), partially melted ($\delta Ar/N_2$), or microbially respired ($\delta^{18}O$ of O_2, $\delta O_2/N_2$, and $\delta O_2/Ar$).

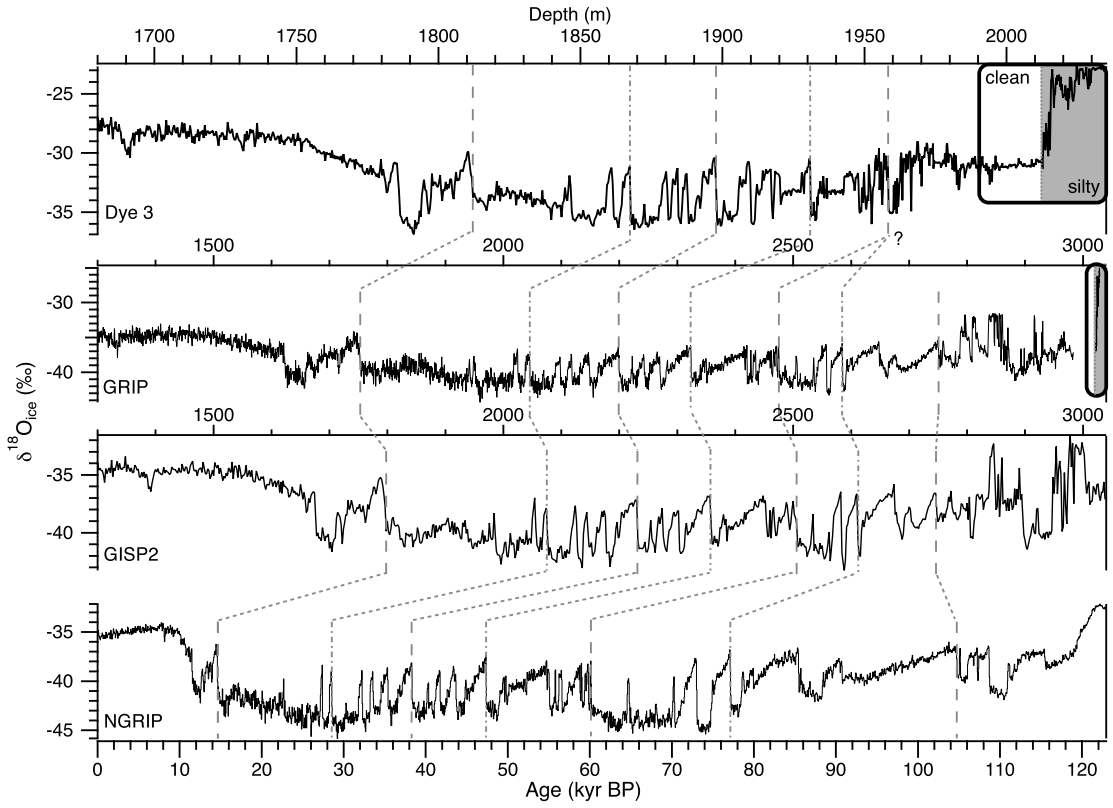

Fig. 2. Comparison of $\delta^{18}O_{ice}$ for Dye-3, GRIP, GISP2, and NGRIP ice cores. Dye-3, GRIP, and GISP2 are plotted on the top axis versus depth. NGRIP is plotted on the bottom axis versus age. Dotted lines show $\delta^{18}O_{ice}$ matching between cores. GRIP and GISP2 are chronologically continuous to ~105 ka, and Dye-3 is chronologically continuous to ~60 ka. The bold boxes highlight the analyzed sections of Dye-3 and GRIP. The shaded portion indicates silty basal ice.

We also date the trapped air from both cores by measuring the paleoatmospheric $\delta^{40}Ar/^{38}Ar$ (Bender et al., 2008), and we present measurements of $^{17}\Delta$ of O_2 (Blunier et al., 2002; Blunier et al., 2012) that help constrain the age of basal Dye-3 ice. These analyses contribute to our understanding of the origin of the basal ice from Dye-3 and GRIP, and how old this ice may be. These results provide useful constraints on the long-term stability of the GIS and models predicting its evolution in response to global change.

2. Methods

Interpreting gas properties requires a correction for gravitational fractionation. This term refers to the fact that, in a diffusive environment, heavy gases and isotopes are progressively enriched with depth according to the barometric equation. The enrichment scales with mass difference (Craig et al., 1988). We measure gravitational enrichment from $\delta^{15}N$ and $\delta^{38}Ar/^{36}Ar$. Gases may also be biased from the atmospheric composition by thermal fractionation. The effect of thermal fractionation is discussed in section 3.2.

2.1. Age reconstruction – Ar-chronometer

We have dated the trapped air of the deepest GRIP and Dye-3 ice by the Ar-isotope method (Bender et al., 2008). The chronometer makes use of the fact that ^{36}Ar and ^{38}Ar have been essentially constant throughout recent geologic time, but ^{40}Ar has been slowly increasing in the atmosphere as a result of the decay of ^{40}K. $\delta^{40}Ar/^{38}Ar$ has been measured in ice cores to 800 ka. Over this period, it has risen at a rate of 0.066 ± 0.007‰/Ma. We precisely measure the $\delta^{40}Ar/^{38}Ar$ of the trapped air and determine the age of the air based on this rate of $\delta^{40}Ar/^{38}Ar$ increase.

The analytical method is similar to that described by Bender et al. (2008). Trapped air was extracted using a wet-melting technique, where ice was melted in an evacuated glass flask. The sample was then equilibrated with meltwater, and the meltwater was removed as outlined by Emerson et al. (1995). The sample gas was then passed through a water trap submerged in liquid N_2, in which residual water and CO_2 were frozen out. Ar was purified from the remaining gases through exposure to a getter which, when activated, reacts with and removes non-noble gases. The remaining gas was captured in a stainless steel tube submerged in liquid helium. After warming to room temperature, the sample was then analyzed on a Finnigan MAT 252 mass spectrometer with collectors specific to ^{36}Ar, ^{38}Ar, and ^{40}Ar.

Samples and air standards (modern air collected from the roof of the Princeton University Geosciences building in New Jersey) were run in three different analytical periods. The standard deviations of samples run in period 1 ($n = 7$) for $\delta^{40}Ar/^{38}Ar$, $\delta^{38}Ar/^{36}Ar$, and $\delta^{40}Ar/^{36}Ar$ were ±0.018‰, ±0.052‰, and ±0.035‰ respectively. For period 2 ($n = 23$), standard deviations were ±0.016‰, ±0.034‰, and ±0.020‰. For period 3 ($n = 7$), standard deviations were ±0.008‰, ±0.023‰, and ±0.019‰. Table 1 indicates in which suite each sample was analyzed.

The term of merit for dating, $\delta^{40}Ar/^{38}Ar_{atm}$ (paleoatmospheric $\delta^{40}Ar/^{38}Ar$), is defined as

$$\delta^{40}Ar/^{38}Ar_{atm} = \delta^{40}Ar/^{38}Ar - 1.002 * \delta^{38}Ar/^{36}Ar \quad (1)$$

The second term corrects for gravitational fractionation. The standard deviation of $\delta^{40}Ar/^{38}Ar_{atm}$ values, normalized to the means of their analysis periods, is ±0.016‰ ($n = 37$). The corresponding age uncertainty is ±250 kyr (1σ) for a single sample. During the first two analysis periods, 12 Holocene-aged ice samples (Newall Glacier ice core) were also analyzed using the same technique (one

Table 1
Dating by Ar- and O_2-isotope composition w.r.t. air. Each line represents a single analysis.

GRIP ice core						
Depth (m)	Analysis (Period)°	$\delta^{40}Ar/^{38}Ar$ (‰)	$\delta^{40}Ar/^{36}Ar$ (‰)	$\delta^{38}Ar/^{36}Ar$ (‰)	$\delta^{40}Ar/^{38}Ar_{atm}$ (‰)	Age (ka)
3020	3	0.746	1.540	0.793	−0.048	710
3020	3	0.762	1.550	0.788	−0.027	390
3022	3	0.675	1.43	0.757	−0.083	1240
3022	3	0.713	1.482	0.77	−0.058	860
3025	3	0.454	0.963	0.509	−0.056	830
3025	–	–	–	–	–	–
3026	3	0.44	0.88	0.44	0	−10
3026	3	0.428	0.896	0.467	−0.039	580

*Shaded section denotes samples from the silty basal ice.
°See Methods.
Analytical uncertainty for a single sample is ±250 ka.

Dye-3 ice core							
Depth (m)	Analysis (Period)°	$\delta^{40}Ar/^{38}Ar$ (‰)	$\delta^{40}Ar/^{36}Ar$ (‰)	$\delta^{38}Ar/^{36}Ar$ (‰)	$\delta^{40}Ar/^{38}Ar_{atm}$ (‰)	Age (ka)	$^{17}\Delta$ of O_2 (per meg)
2004	–	–	–	–	–	–	40.4
2004	–	–	–	–	–	–	29.6
2008	–	–	–	–	–	–	49.1
2008	–	–	–	–	–	–	47.2
2011	1	0.569	1.155	0.586	−0.017	260	–
2011	2	0.617	1.268	0.650	−0.035	530	–
2015	2	0.223	0.436	0.213	0.010	−150	–
2015	–	–	–	–	–	–	–
2019	1	0.238	0.462	0.224	0.014	−210	–
2019	2	0.150	0.285	0.135	0.015	−230	–
2023	–	–	–	–	–	–	36.1
2023	–	–	–	–	–	–	42.6
2031	2	0.196	0.382	0.186	0.010	−150	53.6
2031	–	–	–	–	–	–	48.0
2035	2	0.246	0.473	0.227	0.019	−280	–
2035	–	–	–	–	–	–	–

*Shaded section denotes samples from the silty basal ice.
°See Methods.
Analytical uncertainty for a single sample is ±250 ka.

Newall sample was removed as an outlier) yielding an average age of 130 ± 150 ka (1σ). During the third analysis period, 3 samples inferred to have Holocene air (shallow ice from Mullins Valley, Antarctica with modern air due to cracks in the surface ice, <5 m depth) were analyzed, yielding an average age of 110 ± 230 ka (1σ).

2.2. Age reconstruction – $^{17}\Delta$ of O_2 stratigraphy

A second technique was used to constrain the age of the basal ice at Dye-3, which involved analyzing the $^{17}\Delta$ of O_2 (the triple isotopic composition of O_2), defined as:

$$^{17}\Delta = \left(\ln\left(\delta^{17}O_{atm}+1\right) - 0.516 * \ln\left(\delta^{18}O_{atm}+1\right)\right) \approx \delta^{17}O_{atm} - 0.516 * \delta^{18}O_{atm} \quad (2)$$

The coefficient (0.516) is the fractionation ratio for $^{17}O/^{16}O$ of O_2 relative to $^{18}O/^{16}O$ (Luz et al., 1999). This technique exploits the fact that $^{17}\Delta$ is a measure of the non mass-dependent fractionation of O_2, which originates in O_2–CO_2 exchange in the stratosphere (Luz et al., 1999). $^{17}\Delta$ changes with time in the atmosphere, and the record is known for the past 400 ka from the Vostok, Siple, and GISP2 ice cores (Fig. 3; Blunier et al., 2012). To a first approximation, $^{17}\Delta$ tracks contemporaneous CO_2 (Blunier et al., 2012). $^{17}\Delta$ data are given in per meg where 1 per meg corresponds to 0.001‰.

Given the definition of $^{17}\Delta$, microbial respiration of air (a mass-dependent fractionation process) does not contaminate this record, as it causes $\delta^{17}O_{atm}$ to change at a rate equal to 0.516 times the change in $\delta^{18}O_{atm}$. In contrast, metabolic production or consumption of gases in silty ice alters all other properties used for gas stratigraphy in ice cores, including CO_2, CH_4, and $\delta^{18}O_{atm}$ (paleoatmospheric $\delta^{18}O$ of O_2). This is an important distinction as the basal silty ice of Dye-3 is contaminated by microbial respiration, with CO_2 values observed up to 36,000 ppmv (Souchez et al., 1998); consequently, these gas properties cannot be used for chemostratigraphy. Here, we make use of the fact that sawtooth, 100-kyr glacial–interglacial CO_2 cycles are observed in the $^{17}\Delta$ record (Blunier et al., 2002; Blunier et al., 2012), which can be used to place samples in the context of the global climate state.

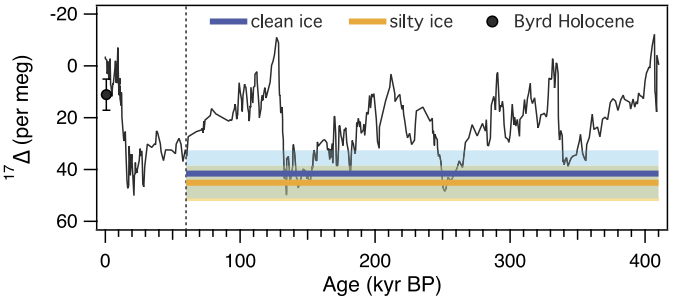

Fig. 3. Mean of $^{17}\Delta$ of O_2 for Dye-3 clean and silty ice plotted versus age. In black, a 3-point smoothing of $^{17}\Delta$ of O_2 for the past 400 ka from Vostok, GISP2, and Siple (Blunier et al., 2012). In yellow, $^{17}\Delta$ of O_2 for silty ice; mean = 45 ± 7 per meg (1σ in light yellow; st. error = ±4 per meg). In blue, $^{17}\Delta$ of O_2 for clean ice; mean = 42 ± 9 per meg (1σ in light blue; st. error = ± 4 per meg). The black circle is the average of Byrd Holocene samples; mean 11 ± 6 per meg (1σ). The dashed line marks 60 ka, the minimum age for the deep ice (see Fig. 2). Mean values for both the clean and silty ice are comparable to glacial maximum values observed for deep ice cores, indicating the air is at least as old as 132 ka.

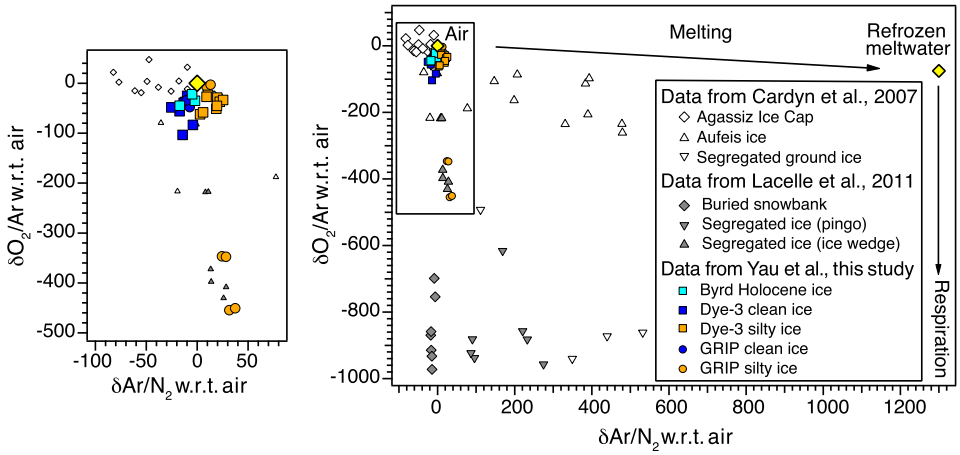

Fig. 4. Right: $\delta Ar/N_2$ vs. $\delta O_2/Ar$ for deep GRIP and Dye-3 ice compared with Holocene ice from Byrd, Antarctica and Agassiz Ice Cap, Canada, and various deposits of wet origin ice. Left: Zoom-in on GRIP and Dye-3 ice. The deepest Dye-3 and GRIP ice have $\delta Ar/N_2$ values similar to that of typical dry densified ice. Some small enrichments in $\delta Ar/N_2$ may be due to regelation of ice or some small mixing with a wet origin ice component. $\delta O_2/N_2$ of the silty GRIP ice samples indicate significant respiration.

The triple isotope composition of oxygen ($^{17}\Delta$) was determined by processing air extracted from ~50 g of ice through a vacuum line connected to a gas chromatograph as per Blunier et al. (2002). $^{17}\Delta$ is calculated by using $\delta^{15}N$ to gravitationally correct both $\delta^{17}O$ and $\delta^{18}O$, which are then used in eqn. (2). The analytical uncertainty in $^{17}\Delta$, based on the analysis of modern air standards, is ± 6 per meg (1σ, $n = 6$). 5 Holocene-aged ice samples (Byrd ice core ~200–500 m depth) were also analyzed using the same sampling technique applied to ice core samples, yielding a Holocene $^{17}\Delta$ of 11 ± 6 per meg (1σ). All $^{17}\Delta$ values are normalized to that of modern air.

2.3. Analyses of the elemental and isotopic composition of O_2, N_2, and Ar

Measurements of the elemental and isotopic composition of air ($\delta^{15}N$, $\delta^{18}O$ of O_2, $\delta Ar/N_2$, $\delta O_2/N_2$, and $\delta O_2/Ar$) were performed using the same wet-melting extraction technique applied for the Ar-dating. In these extractions, ~20 g of ice were used, and samples were passed through a water trap in liquid nitrogen and directly captured in a 12 scc stainless steel tube submerged in liquid helium. The sample was then warmed to room temperature and analyzed on a Finnigan Delta Plus XP mass spectrometer. The standard deviation of modern air standards ($n = 8$), processed as samples, were: $\delta^{15}N = \pm 0.016$‰; $\delta^{18}O$ of $O_2 = \pm 0.023$‰; $\delta Ar/N_2 = \pm 0.24$‰; $\delta O_2/N_2 = \pm 0.45$‰; $\delta O_2/Ar = \pm 0.34$‰. The paleoatmospheric $\delta^{18}O$ of O_2, $\delta^{18}O_{atm}$, is equal to $\delta^{18}O$ corrected for gravitational fractionation: $\delta^{18}O_{atm} = \delta^{18}O - 2.01 * \delta^{15}N$. The standard deviation is ± 0.024‰.

3. Results and discussion

3.1. Characteristics of dry densified ice

Typical dry densified ice has about 100 scc of air per kg (Herron and Langway, 1987). Holocene ice at Summit has a total gas content of ~90 scc/kg, and the total gas content of Holocene Dye-3 ice is somewhat higher (Martinerie et al., 1992).

Dry densified ice is also characterized by near-zero values of $\delta Ar/N_2$, $\delta O_2/N_2$, and $\delta O_2/Ar$ taking ambient air as the reference (Sowers et al., 1989; Bender et al., 1995). Values for $\delta Ar/N_2$ typically range between −10‰ and 0‰ in dry densified ice. These ratios are slightly depleted due to the preferential loss of Ar relative to N_2 during bubble close-off, because Ar atoms are smaller than N_2 molecules (Craig et al., 1988). $\delta Ar/N_2$ values above 0‰ are indicative of partially melted and refrozen ice, as the solubility ratio of Ar/N_2 is approximately 2/1. $\delta O_2/N_2$ and $\delta O_2/Ar$ values of dry densified ice are generally slightly lower than the ratios in air, and are between −25‰ to 0‰ (Sowers et al., 1989; Bender et al., 1995). Depletions below these ratios indicate microbial respiration, which results in the consumption of O_2 (Souchez, 1997). Microbial respiration also results in the enrichment of $\delta^{18}O_{atm}$ (modern air = 0‰; paleo-atmospheric range = −0.4 to +1.4, Dreyfus et al., 2007), as microbes preferentially consume ^{16}O relative to ^{18}O.

In the firn densification process, air is fractionated by gravity, which results in the enrichment of heavier isotopes with depth (Craig et al., 1988; Schwander, 1989). Gravitational fractionation occurs in the firn layer and is preserved in ice once the close-off density is reached. ^{15}N is enriched in the trapped air of dry origin ice, with $\delta^{15}N$ typically between 0.2–0.5‰ (modern air = 0‰), corresponding to a close-off depth of ~40–100 m. This means that for every 20 m depth increase in the firn, $\delta^{15}N$ is enriched by ~0.1‰. If the basal ice of GRIP and Dye-3 is formed by the dry compaction of snow in a climate similar to that of today and at the top of the central ice sheet, we would expect to find the following characteristics: total gas content ~100 scc/kg; $\delta^{15}N$ from ~0.2–0.5‰; values of $\delta^{18}O_{atm}$ within the paleo-atmospheric range (about −0.4‰ to +1.5‰); and Ar/N_2 values slightly below that of modern air.

The presence of liquid water will force elemental ratios of $\delta Ar/N_2$, $\delta O_2/N_2$, and $\delta O_2/Ar$ towards water saturation ratios rather than atmospheric ratios in wet origin ice (Fig. 4). A buried perennial snowbank may have elemental ratios close to that of air, and its trapped air would be gravitationally fractionated. However, the magnitude would be small because of the limited depth, and might be attenuated by convection (Severinghaus et al., 2010). Snowbank air could be thermally fractionated as well. (In thermal fractionation, temperature gradients associated with seasonal temperature fluctuations can fractionate atmospheric ratios and isotopes both negatively and positively; Chapman and Cowling, 1970; Severinghaus et al., 2001.) Low total air contents, elemental ratios drawn towards water saturation ratios, and variable isotopic signatures (reflecting contributions of different processes) would be expected in wet origin basal ice.

3.2. Characteristics of GRIP and Dye-3 basal ice

Table 2 and Figs. 4 and 5 summarize the geochemical data for the trapped air of the deep GRIP and Dye-3 ice. $\delta Ar/N_2$ is plotted vs. $\delta O_2/Ar$ for the GRIP and Dye-3 samples, along with data

Table 2
Gas composition w.r.t. modern air. Each line represents a single analysis.

GRIP ice core

Depth (m)	$\delta O_2/N_2$ (‰)	$\delta O_2/Ar$ (‰)	$\delta Ar/N_2$ (‰)	$\delta^{15}N$ (‰)	$\delta^{18}O_{atm}$ (‰)	$\delta^{18}O_{ice}$ (‰)
3020	−54.65	−47.79	−7.38	0.34	0.87	–
3020	−43.85	−33.88	−10.51	0.37	0.69	–
3022	2.18	−7.37	9.42	0.27	0.38	−34.4
3022	10.36	−2.88	13.08	0.33	0.34	−34.4
3025	−330.55	−346.50	24.30	0.46	4.87	−28.3
3025	−328.92	−347.53	28.35	0.46	4.79	−28.3
3026	−437.32	−454.58	31.51	0.50	5.91	−28.0
3026	−430.15	−450.77	37.32	0.53	5.76	−28.0

*Shaded section denotes samples from the silty basal ice.

Dye-3 ice core

Depth (m)	$\delta O_2/N_2$ (‰)	$\delta O_2/Ar$ (‰)	$\delta Ar/N_2$ (‰)	$\delta^{15}N$ (‰)	$\delta^{18}O_{atm}$ (‰)	$\delta^{18}O_{ice}$ (‰)
1991	−48.75	−37.45	−11.92	0.28	0.36	−31.1
1991	−72.38	−56.12	−17.40	0.29	0.54	−31.1
1999	−116.25	−103.53	−14.38	0.35	1.50	−31.2
1999	−87.25	−83.50	−4.29	0.25	1.25	−31.2
2004	−34.52	−25.04	−9.90	0.27	0.60	−31.0
2004	−72.29	−48.20	−25.49	0.33	0.75	−31.0
2008	−47.31	−37.29	−10.40	0.33	0.51	−31.1
2008	−51.60	−39.06	−13.23	0.30	0.65	−31.1
2011	–	–	–	–	–	−30.6
2011	–	–	–	–	–	−30.6
2014	−11.95	−31.74	20.23	0.16	0.74	−27.9
2014	−9.21	−28.54	19.71	0.17	0.68	−27.9
2015	–	–	–	–	–	−26.6
2015	–	–	–	–	–	−26.6
2019	–	–	–	–	–	−24.0
2019	–	–	–	–	–	−24.0
2023	−13.04	−23.20	10.40	0.20	0.62	−24.5
2023	−17.96	−27.12	9.22	0.13	0.70	−24.5
2027	−15.41	−36.97	22.20	0.10	0.84	−23.4
2027	−8.57	−33.40	25.50	0.07	0.81	−23.4
2031	−32.96	−50.81	18.80	0.16	0.71	−22.9
2031	−26.43	−45.15	19.43	0.07	0.91	−22.9
2035	−59.20	−62.08	2.88	0.11	1.10	−22.8
2035	−52.69	−58.27	5.74	0.12	1.01	−22.8

*Shaded section denotes samples from the silty basal ice.

for various examples of wet origin ice (Fig. 4; Cardyn et al., 2007; Lacelle et al., 2011).

Air trapped in firn from Dye-3 and GRIP have the following characteristics. First, Ar/N_2 ratios are close to atmospheric (Fig. 4). Ratios are slightly elevated in silty GRIP (+37‰) and Dye-3 (+26‰) ice, perhaps due to a small wet origin component (Souchez et al., 1988; Knight, 1997). However, they are nowhere near the saturation value (∼+1000‰). Second, N_2 and Ar isotopes both show normal gravitational enrichments (Fig. 5). The exceptions are in the two deepest dirty GRIP samples, where $\delta^{38}Ar/^{36}Ar$ is much less than $2 \times \delta^{15}N$, and in the silty Dye-3 ice, where the enrichments are only ∼0.1‰ per mass unit. Third, total air content values in silty ice from GRIP and Dye-3 are significantly lower than the overlying clean ice (Table 3; Souchez et al., 1995a, 1998). And fourth, evidence for microbial respiration is clear with $\delta^{18}O_{atm}$ most enriched in samples that are most depleted in O_2 based on the $\delta O_2/Ar$ value (Fig. 5). GRIP silty ice is characterized by unusually large consumption of O_2 and very enriched $\delta^{18}O_{atm}$ values. These observations are all consistent with CO_2 and CH_4 concentrations, and O_2 $\delta^{18}O$ values observed by Souchez et al. (1995b, 2006). The most parsimonious explanation for these observations is that basal ice at GRIP and Dye-3 is composed primarily of dry densified clean ice, with some contribution of silty, wet origin ice. A quantification of mixing components is not attempted here, but has been described in other studies (Souchez et al., 1995a, 1998; Verbeke et al., 2002; Bender et al., 2010).

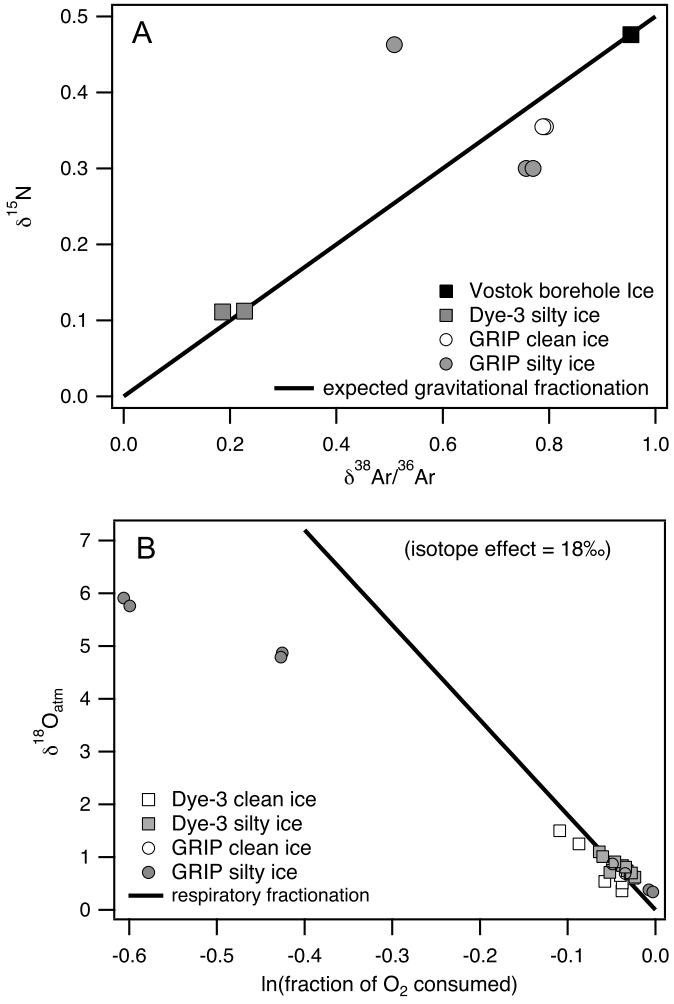

Fig. 5. A. Plot of $\delta^{38}Ar/^{36}Ar$ vs. $\delta^{15}N$. The heavy black line is the expected mass-dependent gravitational fractionation. A Vostok borehole (∼100 m depth) sample illustrates how air from typical ice is fractionated. The Dye-3 silty ice and GRIP clean ice are gravitationally fractionated, though we observe scatter in the deepest silty GRIP samples. B. Plot of the fraction of O_2 consumed (based on the deviation of O_2/Ar from the atmospheric ratio) vs. $\delta^{18}O_{atm}$. The heavy black line is the Rayleigh fractionation relationship assuming a respiratory isotope effect of 18‰. Samples from the deep Dye-3 (clean and silty) and GRIP (clean) ice plot along this line, indicating that some O_2 in the trapped air has been consumed by respiration. GRIP silty basal ice samples show an unusually large degree of consumption. Our $\delta^{18}O$ data are similar to earlier results of Souchez et al. (2006).

3.3. Age constraints on the basal ice of GRIP and Dye-3

Dating of the trapped air reflects the average age of the dry densified glacial ice and locally formed ice, with the components weighted according to their abundance and total gas content. Based on the relatively high total gas content, the local ice component is likely to play a small role in the Ar isotope ages of the most important samples in this study (GRIP at 3022 m and Dye-3 at 2011 m depth). Table 1 summarizes the measured Ar-isotope ages for the deepest ice at GRIP and Dye-3. For GRIP, 4 samples from 3020–3026 m were analyzed. The deepest sample replicated poorly, with one replicate dating to the present. The anomalously young age of this replicate may reflect incorporation of radiogenic ^{40}Ar from outgassing of the local underlying crust, as seen in basal silty ice at GISP2 (Bender et al., 2010). Consequently, we exclude this sample from our discussion of the age of the GRIP basal ice, and infer that the Ar-ages from the basal ice section are lower limits because the trapped air may be contaminated with crustal radiogenic ^{40}Ar. It is possible that wet origin ice could cause Ar

Table 3
Total air content.

GRIP ice core		Dye-3 ice core	
Depth (m)	Air content (scc/g)	Depth (m)	Air content (scc/g)
3022.3	0.098	2010.9	0.081
3022.5	0.084	2012.5	0.089
3022.6	0.068	2014.1	0.069
3022.9	0.077	2014.5	0.089
3023.3	0.087	2015.3	0.090
3023.7	0.077	2016.1	0.053
3024.1	0.080	2016.7	0.067
3024.4	0.068	2018.3	0.061
3024.7	0.070	2021.7	0.068
3025.1	0.063	2022.7	0.060
3025.5	0.058	2023.3	0.075
3025.7	0.074	2024.7	0.053
3026.2	0.065	2025.3	0.065
3026.4	0.068	2027.1	0.056
3026.6	0.072	2027.5	0.057
3027.3	0.059	2028.7	0.064
3027.9	0.051	2029.1	0.053
3028.3	0.048	2029.7	0.053
3028.6	0.048	2031.1	0.052
		2032.1	0.055
		2032.9	0.059
		2033.9	0.047
		2034.7	0.059
		2035.5	0.059
		2035.9	0.052
		2036.7	0.062
		2037.4	0.051
		2037.8	0.036

*Data for GRIP from Souchez et al. (1995a). Data for Dye-3 from Souchez et al. (1998). For Dye-3, Units 1–3, as defined by Souchez et al. (1998), are noted by shading.

isotope ages to be older than the age of the dry densified ice. This influence would only be important if the age of the trapped air from the wet origin ice was not reset by contamination associated with contraction cracks (St. Jean et al., 2011), before it was overridden by dry densified glacial ice. The clean GRIP sample from 3020 m depth dates to 550 ± 170 ka ($n = 2$; 1 st. error), and the remaining silty samples from 3022 m and 3025 m date to 970 ± 140 ka ($n = 3$; 1 st. error). The ^{40}Ar ages for the silty basal ice agree with the ^{10}Be/^{36}Cl age of Willerslev et al. (2007), 950 ± 44 ka. We therefore conclude that the silty basal ice from GRIP certainly dates to well before MIS 11 (430 ka). It is possible that the GRIP silty basal ice dates to the original build-up of the GIS, as originally proposed by Souchez et al. (1994).

For Dye-3, 1 sample was analyzed from the clean section, and 4 from the silty section; one sample was replicated from each section. The average age for the silty basal ice is 210 ± 110 kyr (1 st. error, $n = 2$) in the future. This means that there is excess ^{40}Ar in the basal ice at Dye-3 that is driving the $\delta^{40}\mathrm{Ar}/^{38}\mathrm{Ar}_{\mathrm{atm}}$ value above that of the modern atmosphere. The amount of excess ^{40}Ar far exceeds the amount that could be generated from radiogenic ^{40}Ar produced by just the silt and debris in the ice (weight % between 0.05–0.6%, Olmez et al., 1993). The likely source of excess ^{40}Ar is outgassing of radiogenic ^{40}Ar from the underlying continental crust, as is seen at GISP2 and GRIP (Bender et al., 2010; this work).

The Ar-isotope age for replicates from the clean ice (2011 m) is 400 ± 170 ka (1 st. error, $n = 2$). This result is fully consistent with data in Willerslev et al. (2007) suggesting an age of 400–800 ka for basal ice at Dye-3. However, the large Ar age uncertainty prevents a definitive conclusion at the 95% confidence level that Dye-3 was ice-covered during the Eemian. Consequently, analyses of $^{17}\Delta$ of O_2 are performed to further constrain the age.

For at least the past 400 ka, $^{17}\Delta$ has varied systematically with climate and atmospheric CO_2 (Fig. 3). Interglacial $^{17}\Delta$ typically averages -5 to $+10$ per meg, while glacial values average between $+35$ and $+45$ per meg (Blunier et al., 2002, 2012). With an analytical uncertainty of ± 6 per meg, $^{17}\Delta$ can date trapped air to glacial or interglacial times.

Following Oeschger et al. (1983), we believe that Dye-3 is basically stratigraphically intact back to about 60 ka (Fig. 2). In this view, the δ^{18}O of ice peak at 1932 m corresponds to Interstadial 12 in GISP2 and GRIP (~48 ka). The maximum at 1935 m corresponds to Interstadial 13, and the maximum at 1945 m corresponds to Interstadial 14. At 1956 m and 1958 m in Dye-3, 2 isotope maxima correspond to Interstadial 15 and the short unnumbered interstadial that follows. Then at 1955 m and 1958 m depth, two particularly warm events separated by a cold event correspond to Interstadials 16 and 17 in GISP2 and GRIP. According to these correlations, Dye-3 has an age of 60 ka at 1959 m depth, and deeper ice is presumed to be older.

With this constraint, we use $^{17}\Delta$ to determine the youngest probable age of the trapped air. Fig. 3 shows the results of the $^{17}\Delta$ analyses. 4 clean ice samples had $^{17}\Delta$ values of $+42 \pm 9$ per meg (1σ; st. error $= \pm 4$ per meg). 4 samples of silty ice had $^{17}\Delta$ values of $+45 \pm 7$ per meg (1σ; st. error $= \pm 4$ per meg). These are diagnostic of glacial maximum air and (inferentially) ice (Fig. 3). Given that the minimum age for the deep ice is 60 ka, and that prior to this time, $^{17}\Delta$ values of ~43 per meg were not realized until ~132 ka, we conclude that Dye-3 was ice-covered through the LIG. This interglacial was exceptionally warm. It thus seems likely that the GIS at Dye-3 was intact since the unusually long Marine Isotope Stage 11, and perhaps at earlier times.

4. Conclusions

We have analyzed the concentration and isotopic composition of O_2, N_2 and Ar in trapped gases from clean and silty basal ice from the GISP2 and DYE-3 ice cores. Ar/N_2 ratios, and δ^{15}N of N_2, confirm earlier work (including Souchez et al., 2006) suggesting that trapped gases in silty ice derive primarily from clean, dry densified ice in most samples. ^{40}Ar/^{38}Ar ratios constrain ages with an uncertainty of 150–250 ka for a single sample. Contamination by crustal radiogenic ^{40}Ar make ice ages minimum ages, and in Dye-3 the deepest samples have ages in the future. These limitations notwithstanding, our data have significant implications for the history of the Greenland Ice Sheet.

Analyses of the trapped air from the GRIP and Dye-3 basal ice indicate a relatively resilient GIS. Ar-isotope dating of air from the silty basal ice gives a minimum age for the ice sheet at Summit of 970 ± 140 ka (1 st. error), suggesting that the GIS at Summit survived through MIS 11 despite significant collapse of the GIS (Raymo and Mitrovica, 2012). In addition, evidence that the ice sheet at Dye-3 survived the last interglacial comes from two Ar-isotope dates averaging 400 ± 170 ka (1 st. error). $^{17}\Delta$ stratigraphy further constrains the minimum age to ~132 ka. Ice dating to the last interglacial was not found in the depth interval studied (1991–2035 m), and does not appear to be present at shallower depths, where $\delta^{18}\mathrm{O}_{\mathrm{ice}}$ values do not reach Holocene values (~−28‰; Johnsen et al., 2001). We presume that ice dynamics removed Eemian ice from the Dye-3 site, but the record holds no information about how this might have happened.

It remains a matter of investigation whether the ice sheet at Dye-3 was a part of the main body of the GIS, or whether an ice dome at Southern Greenland was present during the Eemian (Cuffey and Marshall, 2000; Huybrechts, 2002; Tarasov and Peltier, 2003; Lhomme et al., 2005). Our results do not preclude extensive melting of the ice sheet over the LIG, as changes at the margin

as well as in coastal northern Greenland could have been extensive (Born and Nisancioglu, 2012), and the net elevation change at Dye-3 during the LIG is unknown.

Our data indicate that the GIS did not completely melt at Southern Greenland during the Eemian, nor did it completely melt at Summit Greenland during MIS 11. These constraints on the trapped air of basal ice from GRIP and Dye-3 are in line with estimates of the age and stability of the GIS from Willerslev et al. (2007), Colville et al. (2011), and Reyes et al. (2014).

Acknowledgements

This work was supported by the National Science Foundation, Polar Programs, under Grant 0636731, and the BP Amoco – Princeton University Carbon Mitigation Initiative. We are deeply indebted to Jean-Louis Tison and an anonymous reviewer whose comments significantly improved the manuscript.

References

Bamber, J.L., Griggs, J.A., Hurkmans, R., Dowdeswell, J.A., Gogineni, S.P., Howat, I., Mouginot, J., Paden, J., Palmer, S., Rignot, E., Steinhage, D., 2013. A new bed elevation dataset for Greenland. Cryosphere 7, 499–510.

Bender, M., Sowers, T., Lipenkov, V., 1995. On the concentrations of O_2, N_2, and Ar in trapped gases from ice cores. J. Geophys. Res., Atmos. 100, 18651–18660.

Bender, M.L., Barnett, B., Dreyfus, G., Jouzel, J., Porcelli, D., 2008. The contemporary degassing rate of ^{40}Ar from the solid Earth. Proc. Natl. Acad. Sci. USA 105, 8232–8237.

Bender, M.L., Burgess, E., Alley, R.B., Barnett, B., Clow, G.D., 2010. On the nature of the dirty ice at the bottom of the GISP2 ice core. Earth Planet. Sci. Lett. 299, 466–473.

Blunier, T., Barnett, B., Bender, M.L., Hendricks, M.B., 2002. Biological oxygen productivity during the last 60,000 years from triple oxygen isotope measurements. Glob. Biogeochem. Cycles 16. http://dx.doi.org/10.1029/2001gb001460.

Blunier, T., Bender, M.L., Barnett, B., von Fischer, J.C., 2012. Planetary fertility during the past 400 ka based on the triple isotope composition of O_2 in trapped gases from the Vostok ice core. Clim. Past 8, 1509–1526.

Boereboom, T., Samyn, D., Meyer, H., Tison, J.L., 2013. Stable isotope and gas properties of two climatically contrasting (Pleistocene and Holocene) ice wedges from Cape Mamontove Klyk, Laptev Sea, northern Siberia. Cryosphere 7, 31–46.

Born, A., Nisancioglu, K.H., 2012. Melting of Northern Greenland during the last interglaciation. Cryosphere 6, 1239–1250.

Cardyn, R., Clark, I.D., Lacelle, D., Lauriol, B., Zdanowicz, C., Calmels, F., 2007. Molar gas ratios of air entrapped in ice: a new tool to determine the origin of relict massive ground ice bodies in permafrost. Quat. Res. 68, 239–248.

Chapman, S., Cowling, T.G., 1970. The Mathematical Theory of Non-Uniform Gases. Cambridge University Press.

Chappellaz, J., Brook, E., Blunier, T., Malaize, B., 1997. CH_4 and $\delta^{18}O$ of O_2 records from Antarctic and Greenland ice: a clue for stratigraphic disturbance in the bottom part of the Greenland ice core project and the Greenland ice sheet project 2 ice cores. J. Geophys. Res. 102, 26547–26557.

Clark, P.U., Huybers, P., 2009. Global change: interglacial and future sea level. Nature 462, 856–857.

Colville, E.J., Carlson, A.E., Beard, B.L., Hatfield, R.G., Stoner, J.S., Reyes, A.V., Ullman, D.J., 2011. Sr–Nd–Pb isotope evidence for ice-sheet presence on Southern Greenland during the last interglacial. Science 333, 620–623.

Craig, H., Horibe, Y., Sowers, T., 1988. Gravitational separation of gases and isotopes in polar ice caps. Science 242, 1675–1678.

Cuffey, K.M., Marshall, S.J., 2000. Substantial contribution to sea-level rise during the last interglacial from the Greenland ice sheet. Nature 404, 591–594.

Dahl-Jensen, D., Community NEEM, 2013. Eemian interglacial reconstructed from a Greenland folded ice core. Nature 493, 489–494.

Dreyfus, G.B., Parrenin, F., Lemieux-Dudon, B., Durand, G., Masson-Delmotte, V., Jouzel, J., Barnola, J.M., Panno, L., Spahni, R., Tisserand, A., Siegenthaler, U., Leuenberger, M., 2007. Anomalous flow below 2700 m in the EPICA Dome C ice core detected using $\delta^{18}O$ of atmospheric oxygen measurements. Clim. Past 3, 341–353.

Emerson, S., Quay, P.D., Stump, C., Wilbur, D., Schudlich, R., 1995. Chemical tracers of productivity and respiration in the subtropical Pacific Ocean. J. Geophys. Res., Oceans 100, 15873–15887.

Herron, M.M., Langway, C.C., 1980. Firn densification – an empirical model. J. Glaciol. 25, 373–385.

Herron, M.M., Langway, C.C., 1987. Derivation of paleoelevations from total air content of two deep Greenland ice cores. In: The Physical Basis of Ice Sheet Modelling, Proceedings of the Vancouver Symposium. In: IAHS, vol. 170.

Huybrechts, P., 2002. Sea-level changes at the LGM from ice-dynamic reconstructions of the Greenland and Antarctic ice sheets during the glacial cycles. Quat. Sci. Rev. 21, 203–231.

Johnsen, S.J., Dahl-Jensen, D., Gundestrup, N., Steffensen, J.P., Clausen, H.B., Miller, H., Masson-Delmotte, V., Sveinbjornsdottir, A.E., White, J., 2001. Oxygen isotope and palaeotemperature records from six Greenland ice-core stations: camp century, Dye-3, GRIP, GISP2, Renland and NorthGRIP. J. Quat. Sci. 16, 299–307.

Knight, P.G., 1997. The basal ice layer of glaciers and ice sheets. Quat. Sci. Rev. 16, 975–993.

Koerner, R.M., 1989. Ice core evidence for extensive melting of the Greenland ice-sheet in the last interglacial. Science 244, 964–968.

Koerner, R.M., Fisher, D.A., 2002. Ice-core evidence for widespread Arctic glacier retreat in the last interglacial and the early Holocene. In: Wolff, E.W. (Ed.), Ann. Glaciol. 35, 19–24.

Kopp, R.E., Simons, F.J., Mitrovica, J.X., Maloof, A.C., Oppenheimer, M., 2009. Probabilistic assessment of sea level during the last interglacial stage. Nature 462, 863–867.

Lacelle, D., Radtke, K., Clark, I.D., Fisher, D., Lauriol, B., Utting, N., Whyte, L.G., 2011. Geomicrobiology and occluded O_2–CO_2–Ar gas analyses provide evidence of microbial respiration in ancient terrestrial ground ice. Earth Planet. Sci. Lett. 306, 46–54.

Lhomme, N., Clarke, G.K.C., Marshall, S.J., 2005. Tracer transport in the Greenland Ice Sheet: constraints on ice cores and glacial history. Quat. Sci. Rev. 24, 173–194.

Luz, B., Barkan, E., Bender, M.L., Thiemens, M.H., Boering, K.A., 1999. Triple-isotope composition of atmospheric oxygen as a tracer of biosphere productivity. Nature 400, 547–550.

Martinerie, P., Raynaud, D., Etheridge, D.M., Barnola, J.M., Mazaudier, D., 1992. Physical and climatic parameters which influence the air content in polar ice. Earth Planet. Sci. Lett. 112, 1–13.

Oeschger, H., Beer, J., Siegenthaler, U., Stauffer, B., Dansgaard, W., Langway, C.C., 1983. Late Glacial climate history from Ice Cores. In: Paleoclimate Research and Models.

Olmez, I., Fireman, E.L., Langway, C.C., 1993. Trace-elements in basal ice at Dye-3. Atmospheric environment part A–general. Topics 27, 2921–2926.

Raymo, M.E., Mitrovica, J.X., 2012. Collapse of polar ice sheets during the stage 11 interglacial. Nature 483, 453–456.

Reyes, A.V., Carlson, A.E., Beard, B.L., Hatfield, R.G., Stoner, J.S., Winsor, K., Welke, B., Ullman, D.J., 2014. South Greenland ice-sheet collapse during Marine isotope stage 11. Nature 510, 525–528.

Schwander, J., 1989. The transformation of snow to ice and the occlusion of gases. In: Oescer, H., Langway, C. (Eds.), The Environmental Record in Glaciers and Ice Sheets. John Wile, New York.

St. Jean, M., Lauriol, B., Clark, I.D., Lacelle, D., Zdanowicz, C., 2011. Investigation of ice-wedge infilling processes using stable oxygen and hydrogen isotopes, crystallography and occluded gases (O_2, N_2, Ar). Permafr. Periglac. Process. 22, 49–64.

Severinghaus, J.P., Grachev, A., Battle, M., 2001. Thermal fractionation of air in polar firn by seasonal temperature gradients. Geochem. Geophys. Geosyst. 2. http://dx.doi.org/10.1009/2000GC000146.

Severinghaus, J.P., Albert, M.R., Courville, Z.R., Fahnestock, M.A., Kawamura, K., Montzka, S.A., Muhle, J., Scambos, T.A., Shields, E., Shuman, C.A., Suwa, M., Tans, P., Weiss, R.F., 2010. Deep air convection in the firn at a zero-accumulation site, central Antarctica. Earth Planet. Sci. Lett. 293, 359–367.

Souchez, R., Lorrain, R., Tison, J.L., Jouzel, J., 1988. Co-isotopic signature of two mechanisms of basal-ice formation in Arctic outlet glaciers. Ann. Glaciol. 10, 163–166.

Souchez, R., Tison, J.L., Lorrain, R., Lemmens, M., Janssens, L., Stievenard, M., Jouzel, J., Sveinbjornsdottir, A., Johnsen, S.J., 1994. Stable isotopes in the basal silty ice preserved in the Greenland ice sheet at summit; environmental implications. Geophys. Res. Lett. 21, 693–696.

Souchez, R., Janssens, L., Lemmens, M., 1995a. Very low oxygen concentration in basal ice from summit, central Greenland. Geophys. Res. Lett. 22, 2001–2004.

Souchez, R., Lemmens, M., Chappellaz, J., 1995b. Flow-induced mixing in the GRIP basal ice deduced from the CO_2 and CH_4 records. Geophys. Res. Lett. 22, 41–44.

Souchez, R., 1997. The buildup of the ice sheet in central Greenland. J. Geophys. Res., Oceans 102, 26317–26323.

Souchez, R., Bouzette, A., Clausen, H.B., Jonsen, S.J., Jouzel, J., 1998. A stacked mixing sequence at the base of the Dye-3 core, Greenland. Geophys. Res. Lett. 25, 1943–1946.

Souchez, R., Jouzel, J., Landais, A., Chappellaz, J., Lorrain, R., Tison, J.L., 2006. Gas isotopes in ice reveal a vegetated central Greenland during ice sheet invasion. Geophys. Res. Lett. 33, L24503.

Sowers, T., Bender, M., Raynaud, D., 1989. Elemental and isotopic composition of occluded O_2 and N_2 in polar ice. J. Geophys. Res., Atmos. 94, 5137–5150.

Suwa, M., von Fischer, J.C., Bender, M.L., Landais, A., Brook, E.J., 2006. Chronology reconstruction for the disturbed bottom section of the GISP2 and the GRIP ice cores: implications for termination II in Greenland. J. Geophys. Res., Atmos. 111. http://dx.doi.org/10.1029/2005JD006032.

Tarasov, L., Peltier, W.R., 2003. Greenland glacial history, borehole constraints, and Eemian extent. J. Geophys. Res., Solid Earth 108. http://dx.doi.org/10.1029/2001JB001731.

Tison, J.-L., Thorsteinsson, T., Lorrain, R.D., Kipfstuhl, J., 1994. Origin and development of textures and fabrics in basal ice at summit, Central Greenland. Earth Planet. Sci. Lett. 125, 421–437.

Tison, J.-L., Souchez, R., Wolff, E.W., Moore, J.C., Legrand, M.R., de Angelis, M., 1998. Is a periglacial biota responsible for enhanced dielectric response in basal ice from the Greenland ice core project ice core? J. Geophys. Res. 103, 18885–18894.

Verbeke, V., Lorrain, R., Johnsen, S.J., Tison, J., 2002. A multiple-step deformation history of basal ice from the Dye 3 (Greenland) core: new insights from the CO_2 and CH_4 content. Ann. Glaciol. 35, 231–236.

Willerslev, E., Cappellini, E., Boomsma, W., Nielsen, R., Hebsgaard, M.B., Brand, T.B., Hofreiter, M., Bunce, M., Poinar, H.N., Dahl-Jensen, D., Johnsen, S., Steffensen, J.P., Bennike, O., Schwenninger, J.L., Nathan, R., Armitage, S., de Hoog, C.J., Alfimov, V., Christl, M., Beer, J., Muscheler, R., Barker, J., Sharp, M., Penkman, K.E.H., Haile, J., Taberlet, P., Gilbert, M.T.P., Casoli, A., Campani, E., Collins, M.J., 2007. Ancient biomolecules from deep ice cores reveal a forested southern Greenland. Science 317, 111–114.

Yau, A.M., 2014. Extending polar ice core records: studies on the trapped air of glacial ice from Antarctica, Greenland, and the Canadian Arctic. PhD Thesis Dissertation. Princeton University.